Krüppel-like factor 5 regulates wound repair and the innate immune response in human airway epithelial cells

Received for publication, January 28, 2021, and in revised form, June 17, 2021 Published, Papers in Press, July 1, 2021,
https://doi.org/10.1016/j.jbc.2021.100932

Alekh Paranjapye, Monali NandyMazumdar, James A. Browne, Shih-Hsing Leir, and Ann Harris*
From the Department of Genetics and Genome Sciences, Case Western Reserve University, Cleveland, Ohio, USA

Edited by Eric Fearon

A complex network of transcription factors regulates genes involved in establishing and maintaining key biological properties of the human airway epithelium. However, detailed knowledge of the contributing factors is incomplete. Here we characterize the role of Krüppel-like factor 5 (KLF5), in controlling essential pathways of epithelial cell identity and function in the human lung. RNA-seq following siRNA-mediated depletion of KLF5 in the Calu-3 lung epithelial cell line identified significant enrichment of genes encoding chemokines and cytokines involved in the proinflammatory response and also components of the junctional complexes mediating cell adhesion. To determine direct gene targets of KLF5, we defined the cistrome of KLF5 using ChIP-seq in both Calu-3 and 16HBE14o$^-$ lung epithelial cell lines. Occupancy site concordance analysis revealed that KLF5 colocalized with the active histone modification H3K27ac and also with binding sites for the transcription factor CCAAT enhancer-binding protein beta (C/EBPβ). Depletion of KLF5 increased both the expression and secretion of cytokines including IL-1β, a response that was enhanced following exposure to *Pseudomonas aeruginosa* lipopolysaccharide. Calu-3 cells exhibited faster rates of repair after KLF5 depletion compared with negative controls in wound scratch assays. Similarly, CRISPR-mediated KLF5-null 16HBE14o$^-$ cells also showed enhanced wound closure. These data reveal a pivotal role for KLF5 in coordinating epithelial functions relevant to human lung disease.

Genes governing the major biological functions of the human airway epithelium are tightly regulated by a complex network of transcription factors (TFs). This coordination of gene expression is essential in the maintenance of the epithelial cell identity and integrated function of the epithelium. The role of specific factors in lung development and the consequences of misregulation are well characterized. Pioneer TFs such as members of the GATA (1, 2) and FOX (3–5) families are required for the differentiation of endoderm-derived tissues including the lung. An intricate network of TFs and downstream signaling pathways are necessary for lung epithelial specification (6), and many additional TFs support the unique properties of the fully differentiated lung epithelium. The heterodimeric factor activator protein 1 (AP-1) and members of this complex regulate gene expression for many critical processes in lung biology such as the response to external stimuli (7, 8). In addition to their role in coordinating the proinflammatory phenotype, a number of TFs also are essential in the tissue response to wounding, including SAM-pointed domain ETS factor (SPDEF) (9, 10) and ETS homologous factor (EHF) (11–14). The FOXA family members Forkhead box A1 and A2 (FOXA1 and FOXA2) are also involved in the barrier functions of primary human airway epithelium (15).

Here we focus on the transcriptional network controlled by Krüppel-like factor 5 (KLF5) in the airway epithelium. First discovered in the crypt cells of the intestinal epithelium (16), KLF5 is among carboxyl-terminal C2H2 zinc finger transcription factors with roles in cellular proliferation and differentiation (17, 18). Another KLF family member, KLF4, is extensively studied for its role in reprogramming somatic cells into induced pluripotent stem cells (iPSCs) (19). KLF2, KLF4, and KLF5 act in concert to regulate the key transcription factor network controlling embryonic stem cell self-renewal (20–23). KLF5 controls key biological processes in several normal cell and tissue types including muscle (24) and the cardiovascular system (25), and its direct targets also have roles in cancer (26, 27). KLF5 has been implicated in preventing epithelial-to-mesenchymal transition (EMT) in human cells, thus maintaining epithelial characteristics (28, 29). In contrast, little is known about the role of KLF5 in the human airway epithelium. Homozygous KLF5-null mice die from respiratory failure shortly after birth, supporting an essential role for the factor in airway morphogenesis (30). We also found that KLF5 was among the most potent repressors of cystic fibrosis transmembrane conductance regulator (*CFTR*) gene transcription in airway epithelial cells (31), suggesting tasks critical for normal lung function.

Our goal was to determine the gene targets and biological pathways regulated by KLF5 in the human airway epithelium to establish its contribution to the hierarchy of the transcriptional network in this tissue. In order to define the KLF5 transcriptome, we performed RNA-seq following siRNA-mediated depletion. Enriched cellular pathways affected by the reduction of the factor were determined by performing gene ontology (GO) process and gene set enrichment analysis

* For correspondence: Ann Harris, ann.harris@case.edu.
Present address for James A. Browne: Department of Pediatrics, Yale University School of Medicine, New Haven, CT.

on the differentially expressed genes. The cistrome of KLF5 was defined by chromatin immunoprecipitation followed by deep sequencing (ChIP-seq). In addition to determining the genome-wide occupancy of KLF5, we used gene annotation to identify its direct targets. Intersection of the differentially expressed genes with the direct target datasets showed that KLF5 regulates genes involved in several critical functions of the airway epithelium, including cell adhesion and the proinflammatory response. Next, we used functional assays in airway epithelial cells to validate the genomic predictions. Using KLF5 depletion by siRNA and KLF5-null (CRISPR-generated) cell lines, we showed that KLF5 deficiency dysregulated key proinflammatory cytokines and enhanced recovery from wounding in comparison to negative controls or clonal wild-type respectively.

Results

KLF5 regulates key biological processes in the human airway epithelium

To determine the target genes of KLF5 in human lung epithelial cells, we performed RNA-seq on triplicate samples of Calu-3 cells treated with either negative control (NC) siRNA or siRNA specific for KLF5. Using a fold change of ≥1.5 and an adjusted *p*-value threshold of 0.05, we identified 533 upregulated genes and 443 genes that were downregulated (Fig. 1*A*). Among the most significantly upregulated genes were those encoding several chemokines and cytokines such as C-X-C Motif Chemokine Ligand 6 (*CXCL6*), C-C Motif Chemokine Ligand 2 (*CCL2*), and C-X-C Motif Chemokine Ligand 8 (*CXCL8*), also known as IL-8. Also, several genes encoding proteins involved in cell adhesion and tight junction complexes were significantly upregulated, for example, intercellular adhesion molecule 1 (*ICAM1*) and claudin 2 (*CLDN2*). The efficacy of the siRNA treatment was confirmed by a consistent, greater than threefold reduction in *KLF5* transcript abundance (Fig. 1*B*). This result was confirmed at the KLF5 protein level by western blot (Fig. S1). A 2-fold increase in *CFTR* transcript levels (Fig. 1*B*) also confirmed our early observations (31) on the repressive role of KLF5 on the gene in airway epithelial cells. KLF5 depletion also caused a significant downregulation of *SPDEF* and upregulation of *FOXA1* transcripts, two TFs that are well characterized in the transcriptional network of these cells. To further examine the effect of KLF5 depletion on the TF expression landscape, the RNA-seq data were filtered for known human TFs using the v1.01 human TF database (32) (Fig. 1*C*). Twenty-seven TFs were found to be upregulated and 19 were downregulated, with genes encoding major developmental factors such as *NOTCH1*, *RUNX1*, and *RUNX3* among the most significantly downregulated. Next, GO process enrichment analysis was performed for all upregulated DEGs (Fig. 1*D*). Recurrent in both the biological process (BP) and molecular function (MF) ontology terms were enrichments of genes involved in cell adhesion and the inflammatory response. Furthermore, the top cellular compartment (CC) terms were involved in the cell surface and extracellular matrix. A significant proportion of upregulated DEGs were also involved in the extracellular signal-related protein kinase 1 and 2 (ERK1/ERK2) cascade. Gene set enrichment analysis was then performed using the Hallmark database to further classify all genes that were differentially expressed on KLF5 depletion (Fig. 1*E*). When both up- and downregulated genes were assessed simultaneously, significant enrichment for pathways involved in (a) tumor necrosis factor alpha (TNFα) signaling *via* nuclear factor kappa-light-chain-enhancer of activated B cells (NF-κB) and (b) EMT was identified, with some evidence for the enrichment of genes involved in the inflammatory response.

The KLF5 cistrome reveals indirect regulation

The genome-wide occupancy of KLF5 in airway epithelial cells is currently uncharacterized though identification of its direct targets, based upon binding site location within or near gene loci, would be valuable. To address this KLF5 ChIP-seq was performed in replicate in both the Calu-3 and 16HBE14o$^-$ cell lines. Peaks were filtered for read enrichment passing an irreproducible discovery rate threshold of 0.05 and a q value ≥3. We identified a total of 2105 and 3520 significant peaks in Calu-3 and 16HBE14o respectively. Consistent with the biological processes that were impacted upon KLF5 depletion, coincidence of KLF5 sites of occupancy was found in both cell lines at multiple genes involved in cell adhesion, for example, the catenin beta 1 (*CTNNB1*) and epithelial cell adhesion molecule (*EPCAM*) gene loci (Fig. 2*A*, *i* and *ii*). KLF5 was bound primarily at promoters, intergenic regions, and within genes. To determine which of the genes that were differentially expressed on KLF5 depletion were direct targets, we intersected the Calu-3 ChIP-seq dataset with the DEGs identified by RNA-seq (Fig. 2*B*). Among 1221 genes with at least one KLF5 peak within 20kb of the locus, only 64 were differentially downregulated and 52 upregulated (Table S1). GO process enrichment analysis of the overlapping gene sets identified response to external stimulus to be associated with genes upregulated following KLF5 depletion. These results suggest that the extensive alterations in the transcriptome, which were evident upon KLF5 depletion, were largely indirect. Next, the KLF5 IDR peak sets from Calu-3 and 16HBE14o$^-$ were intersected to generate a consensus airway cell ChIP-seq dataset. Although KLF5 was found to bind primarily at promoters or distal intergenic regions, over half of the consensus sites were within 1kb of the gene start site (Fig. S2). Gene annotations for consensus KLF5 peaks were filtered for transcription factors and stratified by location of the KLF5 peak (Fig. 2*C*). In contrast to the relatively equal distribution of KLF5 occupancy between gene promoters and nonpromoter elements, 30 of the 35 transcription factor genes had a KLF5 peak within the 3kb promoter region. Furthermore, the only one of these TFs differentially expressed in the RNA-seq was NF-kappa-B inhibitor zeta (NFKBIZ).

To confirm that KLF5 occupancy directly impacts gene expression *in vitro*, we evaluated the mucin 1 (*MUC1*) gene promoter. *MUC1* is significantly downregulated upon KLF5 depletion and shows a robust peak of KLF5 occupancy within

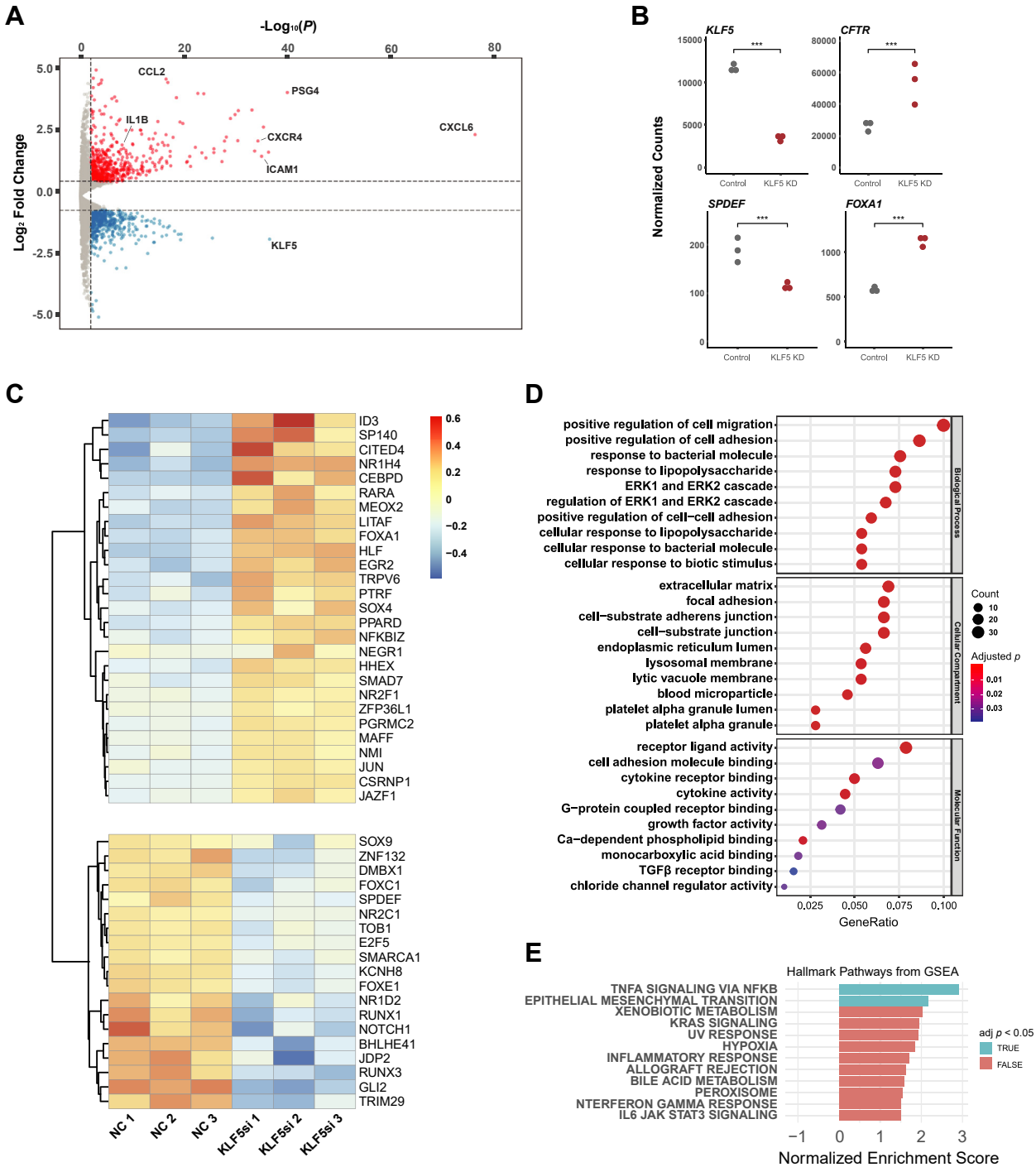

Figure 1. The impact of KLF5 depletion on the transcriptome of Calu-3 cells. Analysis of RNA-seq data. *A*, volcano plot of RNA-seq expression analysis of KLF5-depleted Calu-3 compared with negative control (NC)-treated cells. Plots show -$\log_{10}$ adjusted *p*-value against $\log_2$ fold change. Genes with ≥ 2-fold absolute value fold change passing a 0.01 adjusted *p*-value threshold are noted in *red*. *B*, normalized counts for transcript abundance of KLF5, CFTR, FOXA1, and SPDEF in NC cells and KLF5-depleted cells. *C*, heatmap and dendrogram of all 27 upregulated and 19 downregulated TFs reaching statistical significance. *D*, dot plots for top ten biological process (BP), cellular compartment (CC), and molecular function (MF) gene ontology terms enriched in DEGs upregulated upon KLF5 depletion. *E*, hallmark gene set enrichment analysis of the complete DEG dataset with a normalized enrichment score ≥1.5.

1kb of the transcription start site in the Calu-3 ChIP-seq data. We showed earlier that elements within the *MUC1* promoter controlled gene expression and recruited DNA-binding protein complexes (33). Matrix-scan using Regulatory Sequence Analysis Tools (RSAT) (34) identified a putative KLF5-binding motif in the *MUC1* promoter, corresponding to the ChIP-seq peak at −533 bp to −539 bp with respect to the transcription start site. We performed site-directed mutagenesis to abolish this KLF5 motif in a luciferase reporter gene vector driven by the *MUC1* promoter. The WT and mutant promoter plasmids were transiently transfected into 16HBE14o$^-$ cells and lysates subjected to a dual-luciferase assay (Fig. S3). Mutation of the

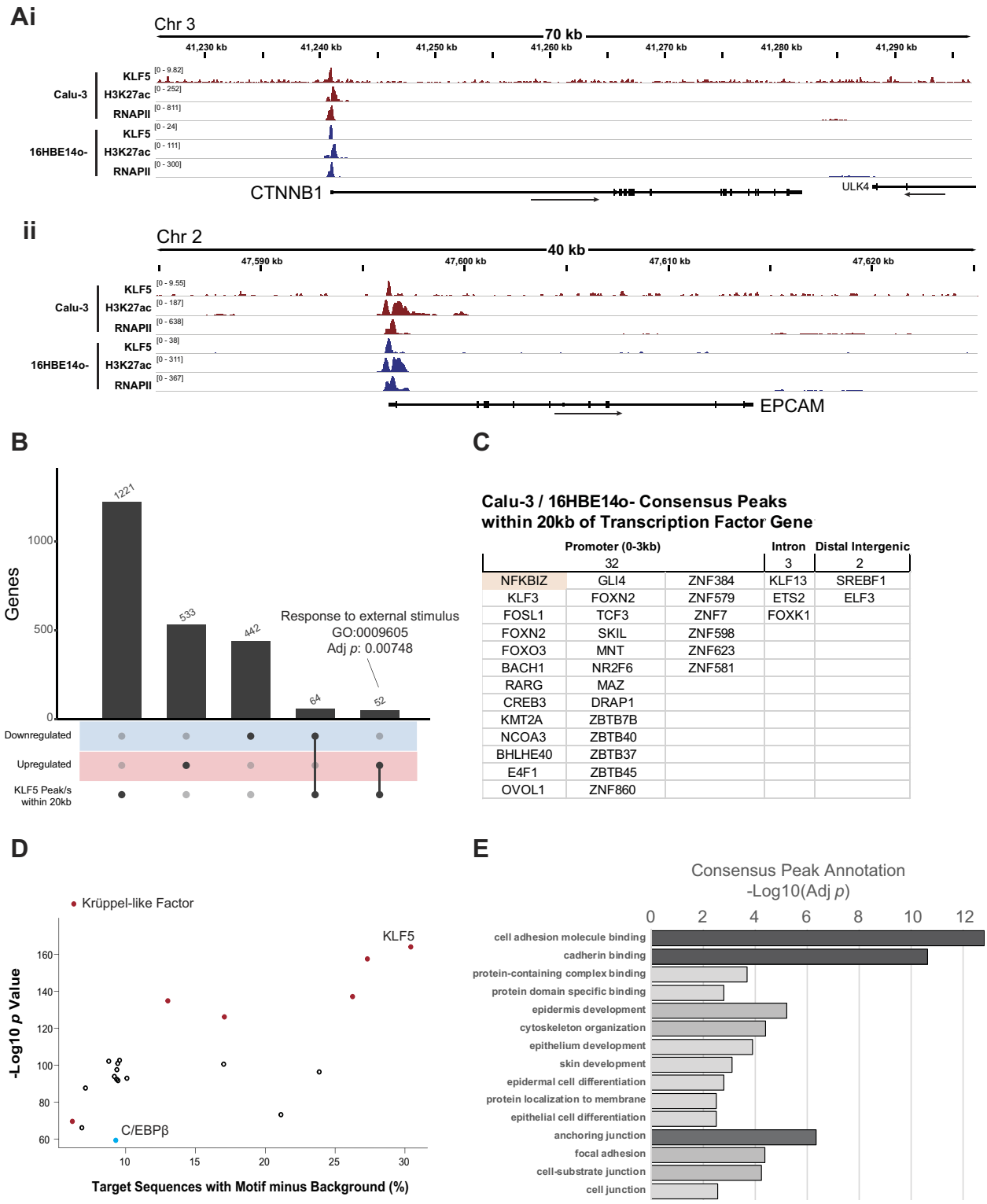

Figure 2. The KLF5 cistrome in Calu-3 and 16HBE14o$^-$ cells. Analysis of ChIP-seq data. *A*, IGV Genome browser graphic shows tracks of KLF5 and H3K27ac ChIP-seq tag counts identified by IDR in Calu-3 (*maroon*) and 16HBE14o$^-$ (*blue*) within 70kb of the CTNNB1 gene (*i*) and 46kb of the EPCAM gene (*ii*). *B*, UpSet plot comparing genes with at least one significant KLF5 Calu-3 peak within 20 kb of the gene body to DEGs identified in the Calu-3 RNA-seq following KLF5 depletion. *C*, table of transcription factors with at least one KLF5 peak shared in Calu-3 and 16HBE14o$^-$ datasets within 20 kb of the gene body. Annotated genes were stratified by the location of the peak. *D*, Scatterplot of the incidence of the top 20 transcription factor binding motifs found under KLF5 peaks shared in Calu-3 and 16HBE14o$^-$. *Red points* indicate motifs for Krüppel-like factors. *E*, gene ontology analysis for all genes with a consensus KLF5 peak within 20kb of the gene body.

KLF5-binding motif significantly reduced the relative luciferase expression compared with WT.

Genome-wide motif analysis was then performed on the airway KLF5 consensus peak set with a 50 bp window around the center of the peak (Fig. 2*D*). The similar DNA-binding motifs for KLFs were the most enriched, as expected in ChIP-seq data for KLF5. Among the top 25 identified, the only motif not belonging to KLFs or members of the AP-1 complex was that of C/EBPβ. The interaction between KLF5 and C/EBPβ has been well characterized in adipocytes (35, 36), though not yet in the airway epithelium. GO analysis was next performed for the closest genes to consensus KLF5 peaks (Fig. 2*E*). As was seen in the RNA-seq dataset, the most significantly enriched terms were those involved in cell adhesion and the cell–cell junctions. These include both the catenin alpha 1 and beta 1 genes (*CTNNA1* and *CTNNB1*) and keratin 18 (*KRT18*). Comparison of the annotated genes in the airway peak sets to those of gastric adenocarcinoma cell lines YCC3 and AGS (37) (GEO: GSE51706) revealed an overlap around 5–10% (Fig. S4*A*). However, GO analysis of annotated genes within 20kb of KLF5 peaks was also significantly enriched for terms related to cadherin binding and cell adhesion. (Fig. S4*B*).

KLF5 binds at active gene promoters and enhancers

To learn more about the *cis* regulatory elements (CREs) bound by KLF5 and identify possible cofactors, we intersected the significant peaks of KLF5 in Calu-3 (Fig. 3*A*, *i*) and 16HBE14o$^-$ (Fig. 3*A*, *ii*) with the ChIP-seq data for the active histone modification H3K27ac and RNA Polymerase II (RNAPII) in the same cell lines (38). In both cell lines, KLF5 peaks were consistently found in regions enriched in H3K27ac with a distinct bimodal distribution around the center of the peak, indicating nucleosome depletion at the TF site. A similar coincidence was found between sites of KLF5 and RNAPII occupancy (Fig. 3*A*, *iii* and *iv*), confirming the activity of the factor at sites of transcription initiation. To assess if the enrichment of the C/EBPβ motif under KLF5 peaks seen in Figure 2*D* coincided with co-occupancy of this factor across the genome, we performed ChIP-seq for C/EBPβ in Calu-3 cells. Direct co-occupancy of these 2 TFs was found at several gene loci. These include differentially expressed genes such as *CFTR* and *NFKBIZ,* as well as mucins 5AC and 5B (*MUC5AC/MUC5B*) and caspase 9 (*CASP9*) (Fig. S5). We then visualized the signal intensity for C/EBPβ binding around KLF5 peaks and included the H3K27ac and RNAPII occupancy data (Fig. 3*B*). A distinct subset of KLF5 peaks overlapped with C/EBPβ sites, significantly correlating with the bimodal distribution of the histone mark and concurrent signal of RNAPII at the center of the peak. To further characterize the co-occupancy of KLF5 and C/EBPβ genome-wide, we intersected the two Calu-3 ChIP-seq peak sets. Binding of the two TFs intersected at 775 sites, corresponding to 33.2% of all KLF5 peaks and 8.02% of C/EBPβ peaks (Fig. 3*C*). Annotation of the closest gene to these co-occupied sites revealed a similar distribution to KLF5 binding alone between promoters and distal intergenic regions.

Cytokine and chemokine expression and secretion are enhanced in KLF5-depleted cells

As shown in Figure 1*A*, we found significant enrichment of genes involved in the immune response among DEGs following KLF5 depletion in Calu-3 cells, for example, *CXCL6* and interleukin 1 beta (*IL1B*). These cytokines are released by the airway epithelium in response to external stimuli such as lipopolysaccharides (LPS) of the cell wall of Gram-negative bacteria (39, 40). To validate whether KLF5 regulated the expression and secretion of these chemokines/cytokines at the basal level and following external stimulus, Calu-3 cells were treated with nontargeting siRNA or siRNA specific for KLF5, followed by treatment of each group with either vehicle control (PBS) or *P. aeruginosa* LPS for 4 h. Chemokine/cytokine expression (CXCL1, CXCL6, and IL-1β) was measured by RT-qPCR (Fig. 4*A*). LPS treatment resulted in a significant increase in the expression of all three cytokines. Consistent with the RNA-seq data, a significant increase in the expression of the *CXCL6* and *IL1B* genes was observed when KLF5 was depleted, with an enhanced increase following LPS treatment. In contrast, CXCL1 levels were unchanged between the control and KLF5-depleted cells. To determine if the change in gene expression coincided with an alteration in IL-1β secretion following KLF5 depletion and LPS treatment, conditioned media was tested using colorimetric sandwich ELISAs (Fig. 4*B*). IL-1β secretion was significantly increased in the media conditioned by KLF5-depleted cells with a greater increase in the media of cells also treated with LPS, consistent with the gene expression changes under the same conditions. Though IL-1β protein levels in the cell lysate also increased slightly after KLF5 depletion, no evidence for a change in the ratio between the precursor and mature forms of IL-1β was evident (data not shown).

Depletion of KLF5 augments wound repair response

Among the most enriched gene sets identified in both the KLF5 depletion RNA-seq and KLF5 ChIP-seq datasets were those involved in focal adhesion, the extracellular matrix, and cadherin binding. Dysregulation of the wound repair response is pivotal to several airway diseases and is also associated with EMT. To evaluate the contribution of KLF5 to coordinating wound repair processes *in vitro*, Calu-3 cells treated with negative control or KLF5-targeted siRNA were grown to confluency. The confluent monolayers were scratched/wounded and subsequently imaged every 3 h for 12 h (Fig. 5*A*). Though no statistically significant difference was observed between treatment groups at the 6-h timepoint, the relative wound size of the KLF5-depleted cells compared with the 3-h timepoint was lower than controls, and this difference reached statistical significance for the 9- and 12-h timepoints (Fig. 5*B*). Thus, depletion of KLF5 was associated with a significantly enhanced speed of wound repair.

To confirm these observations in an orthogonal model system and in a second airway cell line, 16HBE14o$^-$ clonal cell lines without detectable KLF5 protein (KLF5-null) were generated by CRISPR/Cas9 modification. Wound scratch assays were then performed in two wild-type (WT) clonal lines compared with three independent KLF5-null clones (Fig. 3*C*).

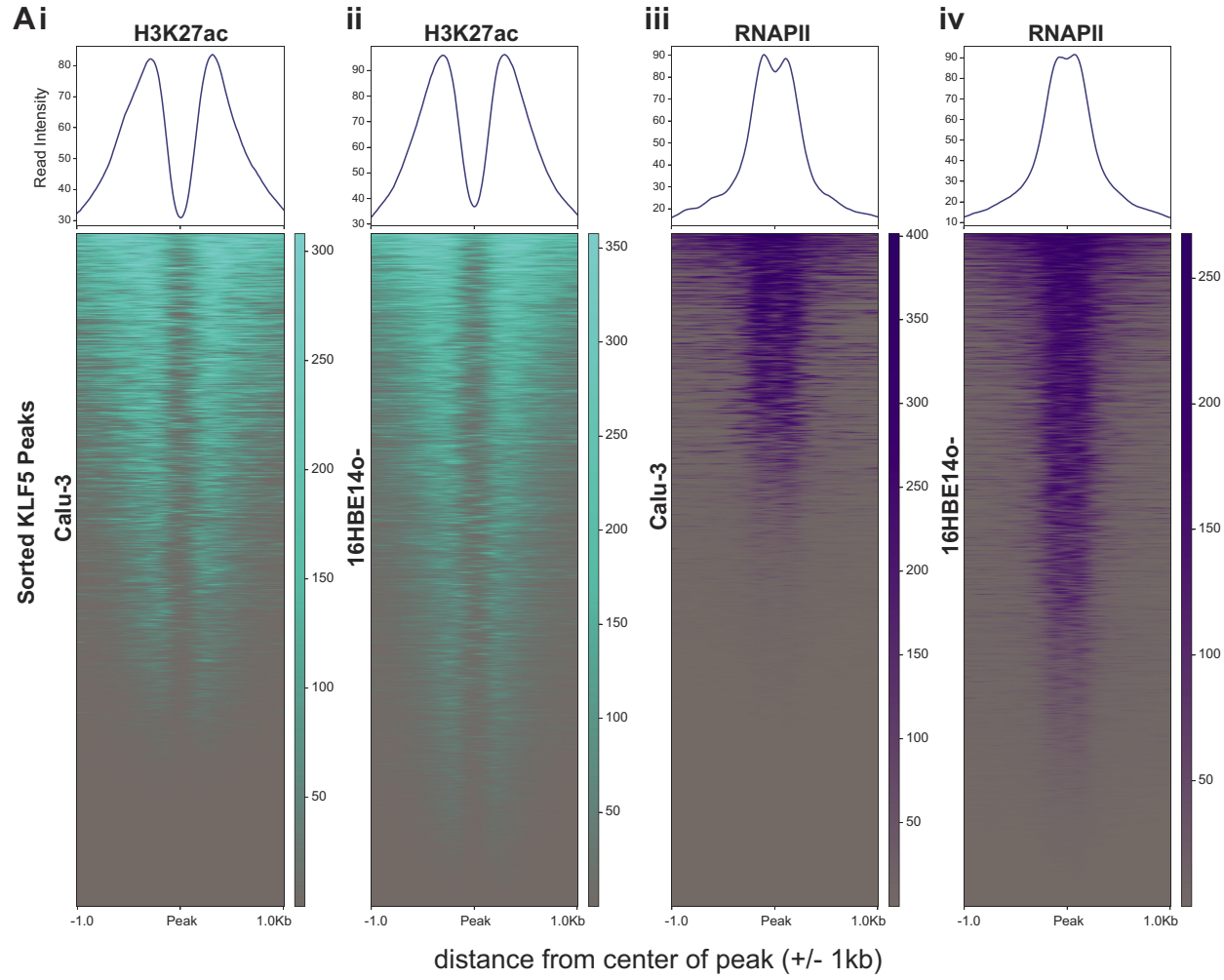

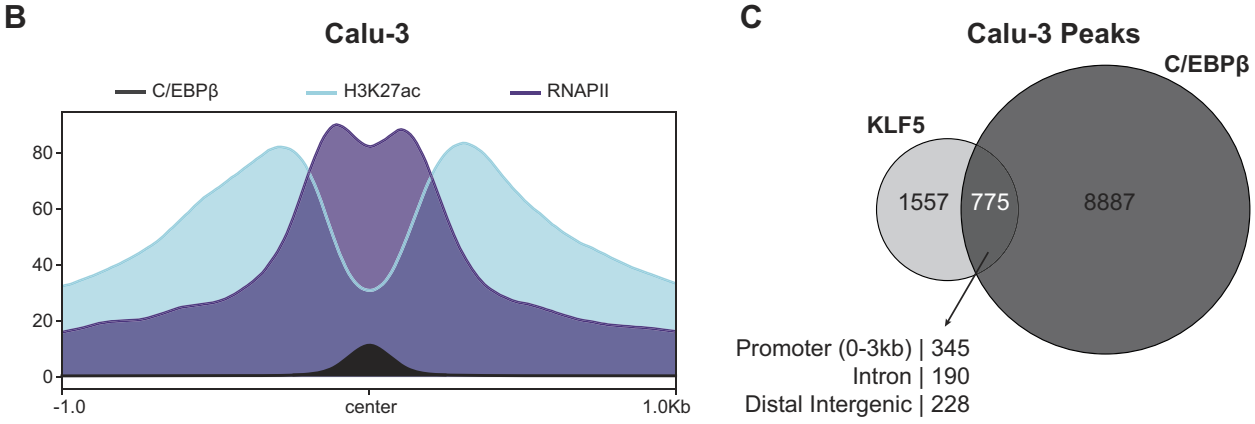

Figure 3. Peaks of KLF5 occupancy coincide with H3K27ac enrichment and C/EBPβ binding sites. *A*, profile plots and heatmaps of ChIP-seq read distribution within 2 kb around significant KLF5 peaks for H3K27ac or RNAPII in Calu-3 (*i*, *iii*), and 16HBE14o$^-$ (*ii*, *iv*). *B*, overlayed profile plot of H3K27ac, RNAPII, or C/EBPβ ChIP-seq read distribution within 2 kb of Calu-3 KLF5 peaks. *C*, Venn diagram of the overlap of genes with at least one site of co-occupancy by both KLF5 and C/EBPβ within 20 kb of the gene body in Calu-3. Location of coincident peaks relative to the closest gene was annotated and stratified.

Loss of KLF5 protein in the KLF5-null clones was confirmed using western blot analysis (Fig. 5*D*). Despite the overall faster rate of wound closure in 16HBE14o$^-$ compared with Calu-3 cells, KLF5-null clonal lines recovered from the scratch at a faster rate than the clonal WT lines, and this difference was statistically significant as early as 6 h post-wounding (Fig. 5*E*).

Importance of KLF5 in primary human bronchial epithelial cells

To confirm that the regulatory roles of KLF5 that were observed in experiments in the Calu-3 and 16HBE14o$^-$ cell lines are equally relevant to primary human airway epithelial cells, we repeated key experiments in primary HBE cells.

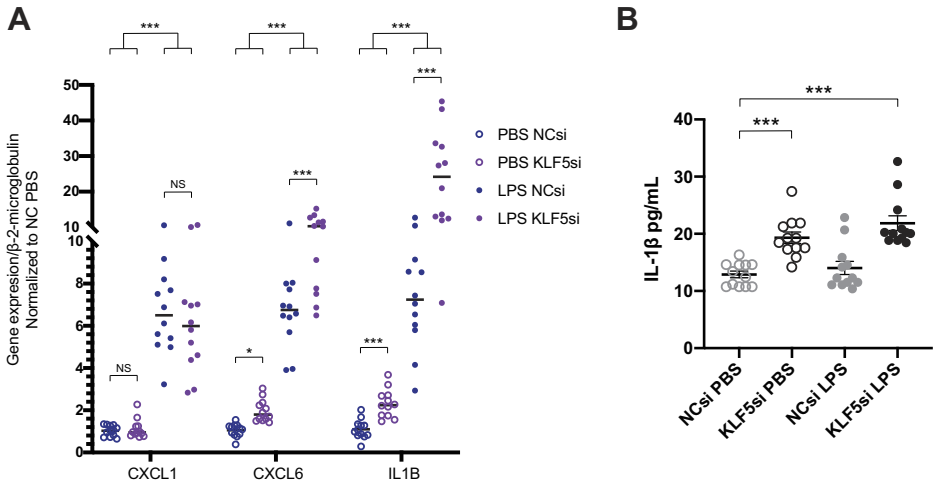

Figure 4. KLF5 depletion in Calu-3 cells alters expression and secretion of IL1B. *A*, gene expression of CXCL1, CXCL6, and IL1B measured by RT-qPCR in Calu-3 cells treated with negative control siRNA or KLF5 depletion followed by exposure to PBS or LPS. *B*, Colorimetric sandwich ELISA measuring secretion of IL-1β in media conditioned by NC and KLF5-depleted Calu-3 cells, followed by PBS or LPS treatment. $^{*}p < 0.01$, $^{***}p < 0.001$, ns, not significant (n = 12) by two-way analysis of variance plus multiple comparisons test (as described in Experimental procedures).

Wound scratch assays were performed in triplicate on HBE cells from two donors after siRNA-mediated depletion of KLF5 compared with an NC siRNA (Fig. 6*A*). As observed in the cell lines, HBE cells depleted for KLF5 recovered from scratch at a significantly faster rate than controls (Fig. 6*B*). The slight lag (15 h instead of 9 h) in significant differences in wound closure between KLF5-depleted cells and controls, when compared with the cell lines, is probably due to the slower growth rate of primary epithelial cells. KLF5 expression does not significantly change during scratch induction or recovery in HBE cells (Fig. S6) (GEO:GSE127696) (41). Differential gene expression in KLF5-depleted HBE cells was assayed by RT-qPCR, focusing on the DEGs identified in the Calu-3 RNA-seq data (Fig. 6*C*). As in Calu-3, the key airway transcription factors SPDEF and FOXA1 were significantly downregulated and upregulated, respectively upon loss of KLF5. We also observed substantial upregulation of ICAM1, CXCL6, and CCL2.

Discussion

The roles of TFs in coordinating the differentiation and development of the lung has been studied extensively (42–45). However, the TF network that maintains the functions of the healthy lung epithelium is less well characterized. Several previous studies focused on members of the Krüppel-like family including KLF4 (46) and KLF15 (47), though examination of the regulatory landscapes of each TF focused primarily on the progression to disease states such as adenocarcinoma. Here, we used genome-wide methods to identify the indirect and potential direct gene targets for KLF5 in these cells. We found that KLF5 regulates genes involved in both the response to external stimuli and cell–cell adhesion, which are two critical functions of the normal lung epithelium with distinct relevance to respiratory health and disease.

The transcriptome in Calu-3 cells showed significant enrichment of genes involved in intercellular junctions and the inflammatory response that were repressed by KLF5. These results are consistent with our previous findings for other members of the TF network such as EHF (14) and FOXA1 (15), where both repress expression of KLF5 (14). The regulatory relationship is further supported by the finding that 46 TFs are differentially expressed upon KLF5 depletion and 37 of these have a peak of KLF5 occupancy close to the gene body. Interestingly, only one of these differentially expressed TFs (NFKBIZ) had KLF5 enrichment at the promoter (Fig. 2*C*), suggesting that KLF5 may have a potent yet indirect role within the TF network. The indirect regulatory potential of KLF5 is further supported by the remarkably low overlap between the direct binding targets identified from our ChIP-seq data in airway epithelial cell lines and the DEG dataset in Calu-3. It is unlikely that this lack of correlation is due poor antibody specificity, as this was validated by western blots of both depletion and CRISPR-null experiments. Further, the reagent has been used elsewhere in ChIP (48, 49).

Direct interaction between KLF5 and other transcription factors plays important roles in other cell types such as with histone deacetylase 1 (HDAC1) in HeLa cells (50) or cyclin-dependent kinase 2 interacting protein (CINP) in the TSU-Pr1 bladder cancer cell line (51). TFs that bind together at *cis*-regulatory elements such as enhancers may also act as cofactors with KLF5. To identify these, we examined the motif enrichment under Calu-3 KLF5 peaks. In addition to the observation of similar motifs for other members of the KLF family, we found enrichment of motifs for the AP-1 family of TFs including c-Jun and JunD. The only other highly enriched motif was that of C/EBPβ, a TF with an important role in the cascade of adipocyte development where it coregulates the expression of genes involved in differentiation, in combination with KLF5 and KLF4 (36). ChIP-seq for C/EBPβ in Calu-3 cells confirmed co-occupancy of this factor with KLF5 at several genes with important roles in airway epithelial biology. As C/EBPβ is recruited to substantially more sites in the genome than KLF5, it may have a more general role at enhancers genome-wide. Nevertheless, comparable enrichment of C/EBPβ and AP-1 motifs under KLF5 peaks supports a possible coregulatory role for C/EBPβ in the epithelium.

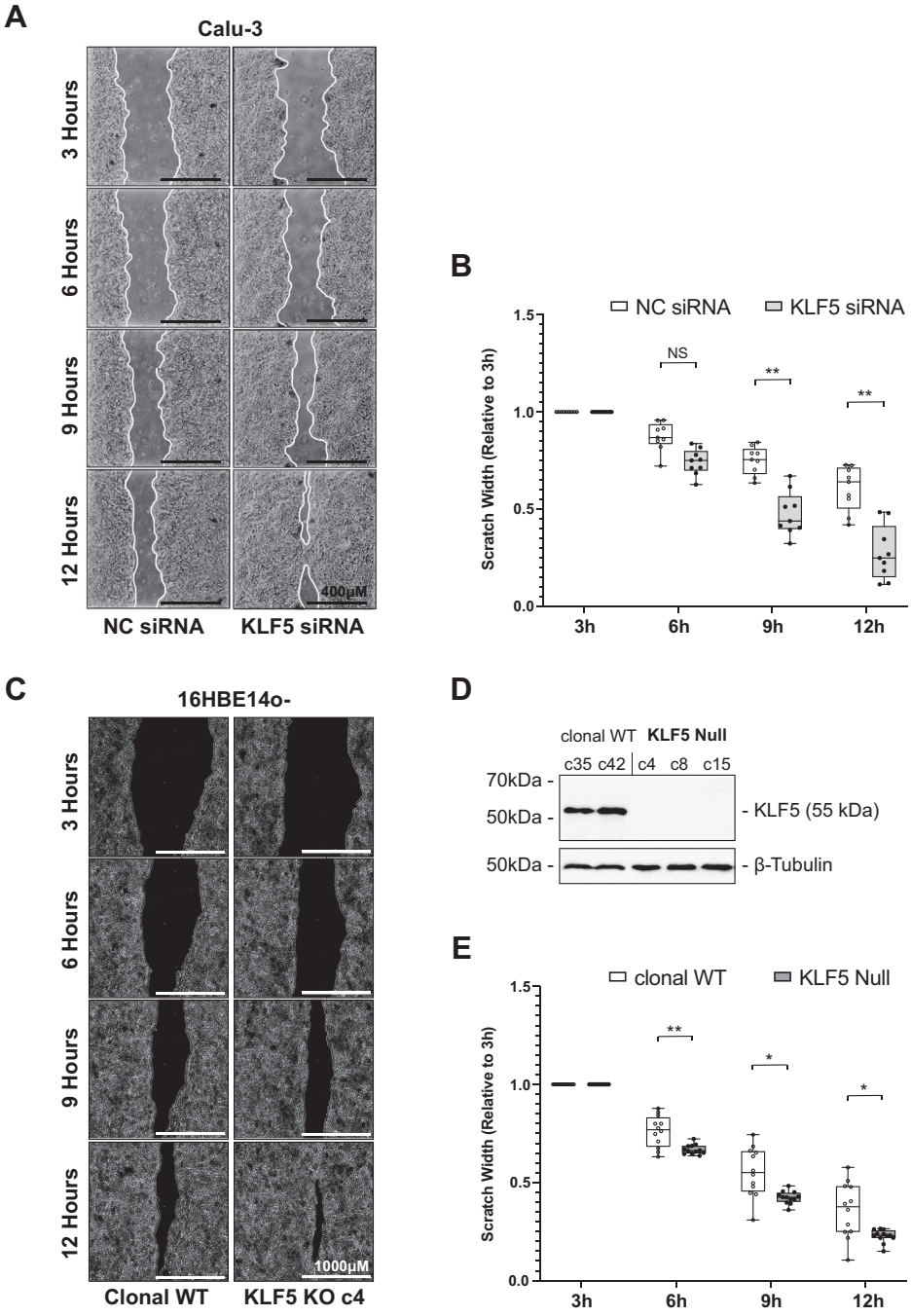

Figure 5. Wound closure rates are enhanced in cells depleted for KLF5 and KLF5-null cells. *A*, representative images of NC and KLF5 siRNA-treated WT Calu-3 cells 3, 6, 9, and 12 h after initial scratch. Outline of wound is traced with a *white line*. Size bar = 400 μm for all panels. *B*, quantification of scratch width in Calu-3 (n = 9 per group). $^{**}p < 0.001$, NS, not significant. *C*, representative images (Lionheart FX) of clonal WT and KLF5-null 16HBE14o$^-$ cells 3, 6, 9, and 12 h after initial scratch. Size bar 1000 μm for all *panels D*. Western blot showing loss of KLF5 protein in KLF5-null CRISPR/cas9 clones compared to clonal wild-type with β-tubulin as a loading control. *E*, quantification of scratch width in 16HBE14o$^-$ clones (n = 12 per group). $^{*}p < 0.01$, $^{**}p < 0.001$. All comparisons were performed using a two-way analysis of variance plus multiple comparisons test.

The consensus KLF5 peaks integrating the cistrome in Calu-3 and 16HBE14o$^-$ were found near genes involved in the cell periphery and cadherin binding as was observed from the transcriptome. The genomic results emphasize the complexity of the regulatory role of KLF5 in the airway epithelium. We found substantial changes in gene expression following depletion of the factor, including genes encoding TFs, yet an almost completely different subset of genes and TFs have KLF5 occupancy near the gene body. Of note, KLF5 binds primarily in regions marked by H3K27ac and occupied by RNAPII. One possibility is that the regulatory role of KLF5 on genes near its binding sites is part of a cascade altering expression of downstream genes. The lack of overlap between TFs with nearby KLF5 peaks and those that are differentially expressed may be due to two or more distinct pathways of regulation. Alternatively, it is possible that KLF5 depletion in Calu-3 does

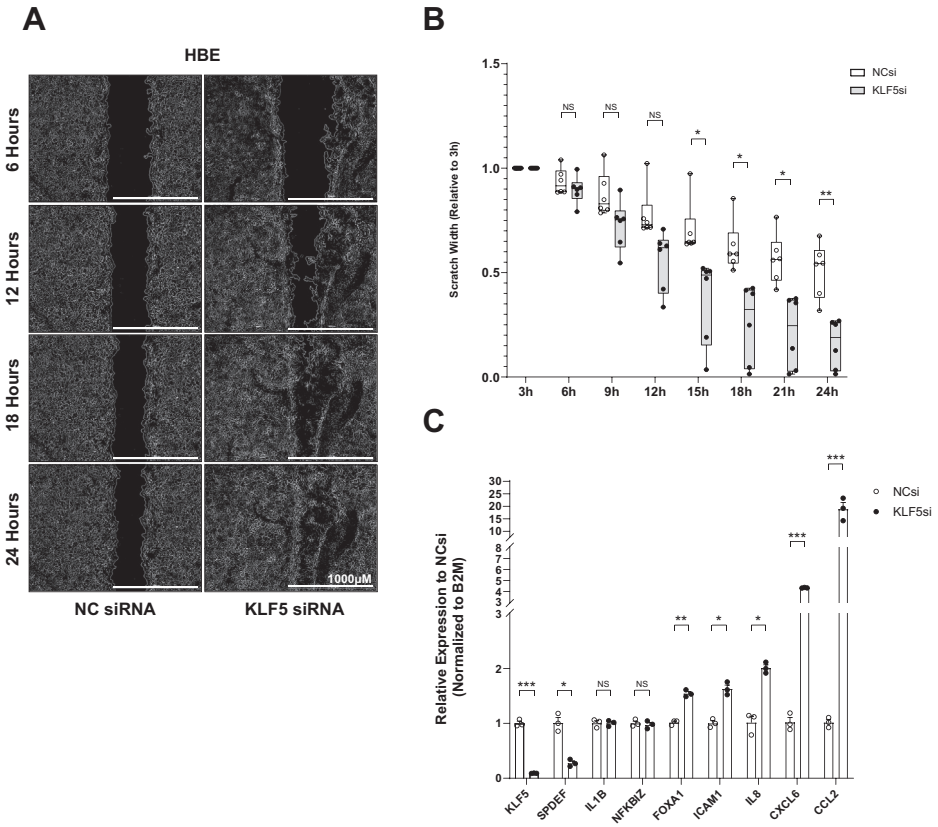

Figure 6. KLF5-depletion enhances wound repair in primary HBE cells. *A*, representative images (Lionheart FX) of NC or KLF5 siRNA depleted HBE cells 6, 12, 18, and 24 h after initial scratch. Size bar =1000 μm for all panels. *B*, quantification of scratch width in HBE cells (n = 6 per group). *C*, gene expression measured by RT-qPCR in HBE cells transfected with NC siRNA or KLF5 siRNA (n = 3). $^{**}p < 0.001$, NS, not significant.

not completely eliminate functional protein. The minimal amounts remaining may be sufficient to occupy sites at some key genes. KLF5 may also act in a tightly monitored feedback loop critical to the airway epithelial cell identity, with the detectable functional consequence of its loss being a shift in the expression of those genes involved in the response to external stimuli and the cell–cell boundary.

To confirm the role of KLF5 on the biological processes identified by genomic methods, we assayed a change in phenotype following depletion of KLF5. As we previously observed with EHF (14), we first assayed the expression and secretion of cytokines and chemokines following KLF5 loss. Subsequent addition of LPS allowed us to further determine if KLF5 plays a role in the epithelial response to stimulus. Other major TFs within the airway epithelial network were shown to play essential roles in innate immunity such as AP-1 (52) as discussed previously and the possible KLF5 cofactor C/EBPβ (53). The dramatic increase in CXCL6 and IL-1β observed in KLF5-depleted cells compared with negative control upon LPS exposure may indicate that in addition to the generally repression of the proinflammatory genes, KLF5 is involved in properly modulating the response to bacterial stimulus. Controlled expression and secretion of IL-1β are critical in the development of the lung (54) and are involved in lung diseases such as chronic obstructive pulmonary disease (COPD) (55). The substantial increase in both expression and secretion of IL-1β highlights the importance of KLF5 in the proinflammatory response of the airway epithelium. Upregulation of *IL1B* upon KLF5 depletion is not accompanied by a change in the relative ratio of the precursor or mature forms of the protein; thus the factor is unlikely to be involved in NLRP3-inflammasome-mediated activation of the cytokine and subsequent proinflammatory response. KLF5 may instead only regulate the NFkB-mediated transcription of IL1B. NLRP3 is not expressed in the airway cells utilized here, but another inflammasome gene, NLRC4, is expressed. This may be more relevant to the proinflammatory response of the airway epithelium, since NLRC4 was found to be essential in the response to *P. aeruginosa* (56, 57). Although we did not find differential expression of *IL1B* in primary HBE, both *CXCL6* and *CCL2* were still significantly upregulated. These results support the role of KLF5 in the regulation of cytokine gene expression in airway epithelium.

Interestingly, IL-1β is also known to promote cell migration in the cancer microenvironment (58); thus in addition to the proinflammatory response effect, the secretion of IL-1β may be involved in the processes of cellular adhesion and the response to wounding. The role of KLF5 in regulating the expression of genes involved in cell adhesion was previously shown in the intestinal epithelium (59), but our observations on the airway epithelium are novel. The integrity of intercellular junctions is closely related to the processes of EMT, and their dysregulation may cause a shift to a mesenchymal cellular identity. In both Calu-3 cells depleted for KLF5 and 16HBE14o$^-$ KLF5-

null cells, we observed significantly increased rates of wound closure. Maintenance of the cell-to-cell contacts and normal barrier function are critical for ion transport and for the integrity of the airway. As genes involved in cell adhesion were both differentially expressed following KLF5 depletion and had peaks of KLF5 occupancy within 20kb of the gene body, our results indicate that this factor may have a pivotal role in maintaining the integrity and health of the airway epithelium. The same response was found in primary HBE, indicating that the response is not unique to cell lines. Primary bronchial epithelial cells better capture the heterogeneity of the human lung surface epithelium and are among the best models for this tissue. The significantly increased rate of scratch closure following loss of KLF5 implicates this factor in the regulation of genes involved in the intercellular matrix, such as differentially expressed ICAM1. Dysregulation of genes involved in this pathway contributes to the defective response to wounding in the context of disease, as observed in cystic fibrosis (60). Significant upregulation of the cytokines CXCL6 and CCL2 in the cell lines and the primary HBE support the role of KLF5 in the proinflammatory response in the context of both healthy epithelium and in disease.

It is of interest to integrate our data into previous studies on the role of KLF5 in other tissues. Although $Klf5^{-/-}$ mouse embryos died before embryonic day 8.5, $Klf5^{+/-}$ mice survived but exhibited abnormal phenotypes in both the vasculature and gastrointestinal track (25). Significant anatomical alterations in these Klf5 deficient mice were accompanied by changes in extracellular matrix components, consistent with our findings of alterations in wound response rate and the expression of genes encoding proteins involved in the cell periphery of human lung epithelium. A role for Klf5 in the response to injury was also found in mouse biliary duct epithelial cells activated by cholestasis (61). Here, Klf5 regulates genes involved in cellular proliferation following cholestatic injury as well as focal adhesion including Laminin A3 (*LAMA3*), which was also significantly downregulated following KLF5 depletion in Calu-3 cells. Of note, earlier work also found KLF5 to have an important role in the LPS-induced proinflammatory response in a human intestinal epithelial cell line (IEC6) (62) and in regulation of *ICAM1* expression, as we observed here in airway epithelial cells. Intersection of the two gastric adenocarcinoma cell lines with the two airway epithelial cell lines identified many shared direct targets for KLF5, though the majority were specific to one cell lineage or the other. GO analysis of the two gastric adenocarcinoma cell lines showed a similar enrichment for those genes at the cell-to-cell periphery. In combination with these observations on other epithelial cells types, our data in human lung epithelial cells provide strong evidence that KLF5 has a critical role in coordinating the establishment and maintenance of the barrier functions of epithelial tissues. The factor regulates multiple genes within the cadherin and laminin families as well as key components of the canonical Wnt signaling pathway including β-Catenin.

Sites of KLF5 occupancy genome-wide in airway epithelial cells coincide with regions marked by active histone marks (H3K27ac) and RNAPII recruitment, thus identifying active promoters and enhancers. However, the factor likely exerts its effects in combination with other TFs at the same elements. In gastric epithelial cells, the key cofactors are probably GATA4/6 and in adipocytes or lung epithelium C/EBPβ is implicated as an important interacting factor. Co-occupancy of regulatory elements could identify a subset of genes that drive the downstream effects seen in RNA-seq, but are not coincident with ChIP-seq targets. The underlying mechanisms may involve chromatin reorganization and three-dimensional structure alterations around coincident binding sites with other TFs and RNAPII, as was found recently for the closely related KLF4 (63). Furthermore, the incidence of this regulatory process at different subsets of gene loci in diverse cell types may underlie the similarity between the pathways, yet discordance of gene targets in epithelia from various tissues.

Experimental procedures

Cell culture

Calu-3 (64) and 16HBE14o$^-$ (65) cells were cultured in Dulbecco's modified Eagle's medium with 10% fetal bovine serum (FBS).

Primary human bronchial epithelial cell culture

Donor-derived primary human bronchial epithelial (HBE) cells were obtained from the Marsico Lung Institute CF Center Tissue Procurement and Cell Culture Core (University of North Carolina [UNC]) and cultured according to the published protocols (66) in accordance with relevant guidelines. The cells were obtained under protocol #03-1396 approved by the University of North Carolina at Chapel Hill Biomedical Institutional Review Board. All donors or their authorized representatives provided informed consent for research use of explanted lungs. This work was also approved by the Case Western Reserve University Institutional Review Board.

KLF5 depletion and RNA-seq

Calu-3 cells were treated with either negative control #2 siRNA (Dharmacon, D-001206-14-05), or KLF5 siRNA (Dharmacon, M-013571-01-0005), each at 30 nM using RNAiMax transfection reagent (Life Technologies). Seventy-two hours after transfection, RNA was isolated from three samples of each treatment using TRIzol (Life Technologies). RNA-seq (SR 50 bp) was performed as described previously (67).

Raw reads were aligned with STAR 2.6 (https://github.com/alexdobin/STAR) (68). Aligned reads were then assigned to genomic features with featureCounts version 1.6.3 in the Subread package (http://subread.sourceforge.net/) (69), and differential gene expression was analyzed using DEseq2 version 1.22.1. (https://www.bioconductor.org/packages/release/bioc/html/DESeq2.html) (70).

Gene ontology and gene set enrichment analyses

Differentially expressed genes were filtered to enrich for genes with a fold change ≥1.5 and Benjamini–Hochberg

adjusted p-value ≤ 0.01. RNA-seq gene lists were read into the gProfiler GO program and database (71). Dot plots for clustered results of each GO term were generated using the genome-wide annotation for human database and mapped using Entrez gene identifiers (72). Statistically significant results were filtered for categories passing a p-value of 0.001 with the Bonferroni correction for multiple testing. Gene set enrichment analysis was performed using the Hallmark human v6.2 database.

ChIP-seq

ChIP-seq was performed using two antibodies against KLF5 (Santa Cruz sc-398470 and rabbit anti-KLF5 kindly donated by Dr Jonathan Katz (73)) or CCAAT enhancer-binding protein beta (C/EBPβ) (Santa Cruz sc-7962) as described previously (13). Raw reads were processed using the ENCODE Transcription Factor and Histone ChIP-Seq processing pipeline (https://github.com/ENCODE-DCC/chip-seq-pipeline2) according to the ENCODE (phase-3) guidelines on the hg19 reference genome. This includes mapping using BWA (74) and peak calling with MACS2 (75). Peak data were filtered using and processed for motif distribution using HOMER (4.7.2q) (http://homer.ucsd.edu/homer/index.html) (76). Consensus peak data were generated using Bedtools intersect (2.29.2) (77), and subsequent annotation was performed using the ChIPseeker package (v3.10) (78). These packages were hosted on the GALAXY platform (79).

Generation of KLF5-null cell line using CRISPR

A single-guide RNA was designed based on Diaferia *et al.* (80) targeting exon 2 of KLF5: 5′-CACCGAAGAACTGGTCTACGACTG-3′ and cloned into pBlueScript (pBS) with a modified multiple cloning site. 16HBE14o$^-$ cells were transfected after 48 h with pMJ920 (wild-type Cas9 plasmid tagged with GFP) (Addgene, plasmid #42234) and pBS containing the KLF5 exon 2 gRNA using Lipofectamine 3000 (Life Technologies). GFP-positive cells were sorted by fluorescence-activated cell sorting and single cells were manually diluted onto 96-well plates. Clones were expanded and screened for homozygous null by western blot and sequencing using primers shown in Table S2.

Transient reporter gene (luciferase) assays

Site-directed mutagenesis was performed on the predicted KLF5 motif in the *MUC1* promoter driving luciferase reporter gene expression in the pGL3B vector (33), using the Agilent QuikChange Lightning Site-Directed Mutagenesis kit. Cells were cotransfected with empty pGL3B, pGL3B containing the WT *MUC1* promoter, or the mutant sequence and a modified pRL *Renilla* luciferase control vector at a 1:10 ratio using Lipofectamine 3000 (Thermo Fischer Scientific). Cells were lysed after 48 h and assayed on a GloMax Navigator (Promega) for firefly and *Renilla* luciferase activity using the Dual-Luciferase Reporter Assay Kit (Promega). Transfections were performed in triplicate in two different passages of 16HBE14o$^-$ cells.

LPS treatment and RT-qPCR

Cells were serum-starved for 24 h and then treated with PBS or 1 μg/ml *Pseudomonas aeruginosa* LPS (Sigma L9143). RNA was collected at 4h using TRIzol, and qRT-PCR was performed using TaqMan Reverse Transcription Reagents kit (LT), oligo $(dT)_{16}$, and primer pairs specific to each gene and SYBR green. β-2-microglobulin was the normalizer (For primers see Table S2). Data were transformed using the delta delta Ct method to calculate the difference between experimental and control values. ANOVA was performed on values before (not shown) and after transformation.

Enzyme-linked immunosorbent assay (ELISA)

Cell culture supernatant from siRNA-transfected cells was collected, cleared by centrifugation at 300*g* for 10 min to remove cell debris, and the supernatant was stored at −80 °C. IL-1β secretion was quantified using the Mini ABTS ELISA Development Kit (PeproTech 900-M95) with no dilution. Standard curves were established using serial dilutions of 1:2 starting with 1000 pg/ml of each target. These assays were performed using the ELISA Buffer Kit (PeproTech 900-K00) according to the manufacturer's protocol.

Wound repair assay

The wound closure assay was performed as described previously (81) on siRNA-treated Calu-3, using a Leica DMi1 microscope (5× objective) and an MC170 HD camera with Las EZ imaging software v3.0.0.47. Wound width was calculated using ImageJ. Experiments on KLF5-null 16HBE14o, clonal wild-type 16HBE14o$^-$ and primary HBE cells were performed using the Lionheart FX automated microscope with a bright field 4× objective. The Biotek scratch assay v1.0 software was used for analysis. All results are from three independent experiments repeated in duplicate for each treatment group, null, or clonal wild-type cell line.

Western blot

KLF5-null and clonal wild-type cells were lysed in NET buffer (10 mM Tris-HCl, pH 7.5, 150 mM NaCl, 5 mM EDTA, 1% Triton X-100, 1X Sigma Protease Inhibitor), and proteins were analyzed by standard methods. The antibodies used were specific for KLF5 (sc-398470), β-tubulin (T4026, Sigma-Aldrich), or IL-1β (12242S, Cell Signaling).

Data availability

KLF5 and C/EBPβ Genome-wide data are deposited at GEO:GSE164853. H3K27ac and RNAPII Genome-wide data are deposited at GEO:GSE132808.

Supporting information—This article contains supporting information.

Acknowledgments—We thank Dr P. Faber and staff at the University of Chicago Genomics Core for all deep sequencing, Dr Sara L. Fossum and Michael J. Mutolo for their assistance in generating the

Calu-3 H3K27Ac and KLF5 ChIP-seq data, Dr Jonathan Katz, University of Pennsylvania, for the rabbit KLF5 antibody (73), and Dr Scott Randell and colleagues at The Marsico Lung Institute Tissue Procurement and Cell Culture Core, for donor-derived HBE cultures (supported in part by CFF Grant BOUCHE15RO and NIH grant DK065988).

Author contributions—A. P. and A. H. conceptualization; A. P., M. N., J. A. B., S.-H. L., and A. H. data curation; A. P. and A. H. formal analysis; A. H. funding acquisition; A. P., M. N., J. A. B., and S.-H. L. investigation; A. P., M. N., J. A. B., and S.-H. L. methodology; A. H. project administration; A. H. supervision; A. P., J. A. B., S.-H. L., and A. H. validation; A. P. visualization; A. P. and A. H. writing-original draft; A. P, M. N., J. A. B., S.-H. L., and A. H. writing-review and editing

Funding and additional information—This work was supported by the National Institutes of Health (R01 HL094585; R01 HL117843; [A. H.]; T32 GM008056 [A. P.]) and the Cystic Fibrosis Foundation (Harris 16G0, 15/17XX0 and 18P0 [A. H.]). The funders had no role in the design of the study, in the collection, analyses, or interpretation of the data, in the writing of the manuscript, or in the decision to publish the results. The content is solely the responsibility of the authors and does not necessarily represent the official views of the National Institutes of Health.

Conflict of interest—The authors declare that they have no conflicts of interest with the contents of this article.

Abbreviations—The abbreviations used are: AP-1, activator protein 1; CFTR, cystic fibrosis transmembrane conductance regulator; ChIP-seq, chromatin immunoprecipitation followed by deep sequencing; CINP, cyclin-dependent kinase 2 interacting protein; C/EBPβ, CCAAT/enhancer binding protein beta; EHF, ETS homologous factor; ELISA, enzyme-linked immunosorbent assay; EMT, epithelial-to-mesenchymal transition; GO, gene ontology; HBE, human bronchial epithelial; HDAC1, histone deacetylase 1; KLF, Krüppel-like factor; LPS, lipopolysaccharide; RSAT, Regulatory Sequence Analysis Tools; SPDEF, SAM-pointed domain ETS factor; TF, transcription factor.

References

1. Lentjes, M. H., Niessen, H. E., Akiyama, Y., de Bruine, A. P., Melotte, V., and van Engeland, M. (2016) The emerging role of GATA transcription factors in development and disease. *Expert Rev. Mol. Med.* **18**, e3
2. Tremblay, M., Sanchez-Ferras, O., and Bouchard, M. (2018) GATA transcription factors in development and disease. *Development* **145**
3. Wan, H., Kaestner, K. H., Ang, S. L., Ikegami, M., Finkelman, F. D., Stahlman, M. T., Fulkerson, P. C., Rothenberg, M. E., and Whitsett, J. A. (2004) Foxa2 regulates alveolarization and goblet cell hyperplasia. *Development* **131**, 953–964
4. Wan, H., Dingle, S., Xu, Y., Besnard, V., Kaestner, K. H., Ang, S. L., Wert, S., Stahlman, M. T., and Whitsett, J. A. (2005) Compensatory roles of Foxa1 and Foxa2 during lung morphogenesis. *J. Biol. Chem.* **280**, 13809–13816
5. Besnard, V., Wert, S. E., Kaestner, K. H., and Whitsett, J. A. (2005) Stage-specific regulation of respiratory epithelial cell differentiation by Foxa1. *Am. J. Physiol. Lung Cell Mol. Physiol.* **289**, L750–L759
6. Rankin, S. A., and Zorn, A. M. (2014) Gene regulatory networks governing lung specification. *J. Cell Biochem.* **115**, 1343–1350
7. Reddy, S. P., and Mossman, B. T. (2002) Role and regulation of activator protein-1 in toxicant-induced responses of the lung. *Am. J. Physiol. Lung Cell Mol. Physiol.* **283**, L1161–L1178
8. Mossman, B. T., Lounsbury, K. M., and Reddy, S. P. (2006) Oxidants and signaling by mitogen-activated protein kinases in lung epithelium. *Am. J. Respir. Cell Mol. Biol.* **34**, 666–669
9. Korfhagen, T. R., Kitzmiller, J., Chen, G., Sridharan, A., Haitchi, H. M., Hegde, R. S., Divanovic, S., Karp, C. L., and Whitsett, J. A. (2012) SAM-pointed domain ETS factor mediates epithelial cell-intrinsic innate immune signaling during airway mucous metaplasia. *Proc. Natl. Acad. Sci. U. S. A.* **109**, 16630–16635
10. Rajavelu, P., Chen, G., Xu, Y., Kitzmiller, J. A., Korfhagen, T. R., and Whitsett, J. A. (2015) Airway epithelial SPDEF integrates goblet cell differentiation and pulmonary Th2 inflammation. *J. Clin. Invest.* **125**, 2021–2031
11. Tugores, A., Le, J., Sorokina, I., Snijders, A. J., Duyao, M., Reddy, P. S., Carlee, L., Ronshaugen, M., Mushegian, A., Watanaskul, T., Chu, S., Buckler, A., Emtage, S., and McCormick, M. K. (2001) The epithelium-specific ETS protein EHF/ESE-3 is a context-dependent transcriptional repressor downstream of MAPK signaling cascades. *J. Biol. Chem.* **276**, 20397–20406
12. Silverman, E. S., Baron, R. M., Palmer, L. J., Le, L., Hallock, A., Subramaniam, V., Riese, R. J., McKenna, M. D., Gu, X., Libermann, T. A., Tugores, A., Haley, K. J., Shore, S., Drazen, J. M., and Weiss, S. T. (2002) Constitutive and cytokine-induced expression of the ETS transcription factor ESE-3 in the lung. *Am. J. Respir. Cell Mol. Biol.* **27**, 697–704
13. Fossum, S. L., Mutolo, M. J., Yang, R., Dang, H., O'Neal, W. K., Knowles, M. R., Leir, S. H., and Harris, A. (2014) Ets homologous factor regulates pathways controlling response to injury in airway epithelial cells. *Nucleic Acids Res.* **42**, 13588–13598
14. Fossum, S. L., Mutolo, M. J., Tugores, A., Ghosh, S., Randell, S. H., Jones, L. C., Leir, S. H., and Harris, A. (2017) Ets homologous factor (EHF) has critical roles in epithelial dysfunction in airway disease. *J. Biol. Chem.* **292**, 10938–10949
15. Paranjapye, A., Mutolo, M. J., Ebron, J. S., Leir, S. H., and Harris, A. (2020) The FOXA1 transcriptional network coordinates key functions of primary human airway epithelial cells. *Am. J. Physiol. Lung Cell Mol. Physiol.* **319**, L126–L136
16. Conkright, M. D., Wani, M. A., Anderson, K. P., and Lingrel, J. B. (1999) A gene encoding an intestinal-enriched member of the Kruppel-like factor family expressed in intestinal epithelial cells. *Nucleic Acids Res.* **27**, 1263–1270
17. Presnell, J. S., Schnitzler, C. E., and Browne, W. E. (2015) KLF/SP transcription factor family evolution: Expansion, diversification, and innovation in eukaryotes. *Genome Biol. Evol.* **7**, 2289–2309
18. Bialkowska, A. B., Yang, V. W., and Mallipattu, S. K. (2017) Kruppel-like factors in mammalian stem cells and development. *Development* **144**, 737–754
19. Takahashi, K., and Yamanaka, S. (2006) Induction of pluripotent stem cells from mouse embryonic and adult fibroblast cultures by defined factors. *Cell* **126**, 663–676
20. Jiang, J., Chan, Y. S., Loh, Y. H., Cai, J., Tong, G. Q., Lim, C. A., Robson, P., Zhong, S., and Ng, H. H. (2008) A core Klf circuitry regulates self-renewal of embryonic stem cells. *Nat. Cell Biol.* **10**, 353–360
21. Aksoy, I., Giudice, V., Delahaye, E., Wianny, F., Aubry, M., Mure, M., Chen, J., Jauch, R., Bogu, G. K., Nolden, T., Himmelbauer, H., Xavier Doss, M., Sachinidis, A., Schulz, H., Hummel, O., *et al.* (2014) Klf4 and Klf5 differentially inhibit mesoderm and endoderm differentiation in embryonic stem cells. *Nat. Commun.* **5**, 3719
22. Zhao, T., Liu, C., and Chen, L. (2015) Roles of Klf5 acetylation in the self-renewal and the differentiation of mouse embryonic stem cells. *PLoS One* **10**, e0138168
23. Parisi, S., Cozzuto, L., Tarantino, C., Passaro, F., Ciriello, S., Aloia, L., Antonini, D., De Simone, V., Pastore, L., and Russo, T. (2010) Direct targets of Klf5 transcription factor contribute to the maintenance of mouse embryonic stem cell undifferentiated state. *BMC Biol.* **8**, 128
24. Watanabe, N., Kurabayashi, M., Shimomura, Y., Kawai-Kowase, K., Hoshino, Y., Manabe, I., Watanabe, M., Aikawa, M., Kuro-o, M., Suzuki, T., Yazaki, Y., and Nagai, R. (1999) BTEB2, a Kruppel-like transcription factor, regulates expression of the SMemb/Nonmuscle myosin heavy chain B (SMemb/NMHC-B) gene. *Circ. Res.* **85**, 182–191

25. Shindo, T., Manabe, I., Fukushima, Y., Tobe, K., Aizawa, K., Miyamoto, S., Kawai-Kowase, K., Moriyama, N., Imai, Y., Kawakami, H., Nishimatsu, H., Ishikawa, T., Suzuki, T., Morita, H., Maemura, K., *et al.* (2002) Kruppel-like zinc-finger transcription factor KLF5/BTEB2 is a target for angiotensin II signaling and an essential regulator of cardiovascular remodeling. *Nat. Med.* **8**, 856–863
26. Miyamoto, S., Suzuki, T., Muto, S., Aizawa, K., Kimura, A., Mizuno, Y., Nagino, T., Imai, Y., Adachi, N., Horikoshi, M., and Nagai, R. (2003) Positive and negative regulation of the cardiovascular transcription factor KLF5 by p300 and the oncogenic regulator SET through interaction and acetylation on the DNA-binding domain. *Mol. Cell Biol.* **23**, 8528–8541
27. Li, J., Zhang, B., Liu, M., Fu, X., Ci, X., A, J., Fu, C., Dong, G., Wu, R., Zhang, Z., Fu, L., and Dong, J. T. (2020) KLF5 is crucial for androgen-AR signaling to transactivate genes and promote cell proliferation in prostate cancer cells. *Cancers (Basel)* **12**, 748
28. Zhang, B., Zhang, Z., Xia, S., Xing, C., Ci, X., Li, X., Zhao, R., Tian, S., Ma, G., Zhu, Z., Fu, L., and Dong, J. T. (2013) KLF5 activates microRNA 200 transcription to maintain epithelial characteristics and prevent induced epithelial-mesenchymal transition in epithelial cells. *Mol. Cell Biol.* **33**, 4919–4935
29. Nakaya, T., Ogawa, S., Manabe, I., Tanaka, M., Sanada, M., Sato, T., Taketo, M. M., Nakao, K., Clevers, H., Fukayama, M., Kuroda, M., and Nagai, R. (2014) KLF5 regulates the integrity and oncogenicity of intestinal stem cells. *Cancer Res.* **74**, 2882–2891
30. Wan, H., Luo, F., Wert, S. E., Zhang, L., Xu, Y., Ikegami, M., Maeda, Y., Bell, S. M., and Whitsett, J. A. (2008) Kruppel-like factor 5 is required for perinatal lung morphogenesis and function. *Development* **135**, 2563–2572
31. Mutolo, M. J., Leir, S. H., Fossum, S. L., Browne, J. A., and Harris, A. (2018) A transcription factor network represses CFTR gene expression in airway epithelial cells. *Biochem. J.* **475**, 1323–1334
32. Lambert, S. A., Jolma, A., Campitelli, L. F., Das, P. K., Yin, Y., Albu, M., Chen, X., Taipale, J., Hughes, T. R., and Weirauch, M. T. (2018) The human transcription factors. *Cell* **172**, 650–665
33. Shiraga, T., Winpenny, J. P., Carter, E. J., McCarthy, V. A., Hollingsworth, M. A., and Harris, A. (2005) MZF-1 and DbpA interact with DNase I hypersensitive sites that correlate with expression of the human MUC1 mucin gene. *Exp. Cell Res.* **308**, 41–52
34. Nguyen, N. T. T., Contreras-Moreira, B., Castro-Mondragon, J. A., Santana-Garcia, W., Ossio, R., Robles-Espinoza, C. D., Bahin, M., Collombet, S., Vincens, P., Thieffry, D., van Helden, J., Medina-Rivera, A., and Thomas-Chollier, M. (2018) RSAT 2018: Regulatory sequence analysis tools 20th anniversary. *Nucleic Acids Res.* **46**, W209–W214
35. Oishi, Y., Manabe, I., Tobe, K., Tsushima, K., Shindo, T., Fujiu, K., Nishimura, G., Maemura, K., Yamauchi, T., Kubota, N., Suzuki, R., Kitamura, T., Akira, S., Kadowaki, T., and Nagai, R. (2005) Kruppel-like transcription factor KLF5 is a key regulator of adipocyte differentiation. *Cell Metab.* **1**, 27–39
36. Cervantes-Camacho, C., Beltran-Langarica, A., Ochoa-Uribe, A. K., Marsch-Moreno, M., Ayala-Sumuano, J. T., Velez-delValle, C., and Kuri-Harcuch, W. (2015) The transient expression of Klf4 and Klf5 during adipogenesis depends on GSK3beta activity. *Adipocyte* **4**, 248–255
37. Chia, N. Y., Deng, N., Das, K., Huang, D., Hu, L., Zhu, Y., Lim, K. H., Lee, M. H., Wu, J., Sam, X. X., Tan, G. S., Wan, W. K., Yu, W., Gan, A., Tan, A. L., *et al.* (2015) Regulatory crosstalk between lineage-survival oncogenes KLF5, GATA4 and GATA6 cooperatively promotes gastric cancer development. *Gut* **64**, 707–719
38. NandyMazumdar, M., Yin, S., Paranjapye, A., Kerschner, J. L., Swahn, H., Ge, A., Leir, S. H., and Harris, A. (2020) Looping of upstream cis-regulatory elements is required for CFTR expression in human airway epithelial cells. *Nucleic Acids Res.* **48**, 3513–3524
39. Edelman, D. A., Jiang, Y., Tyburski, J. G., Wilson, R. F., and Steffes, C. P. (2007) Cytokine production in lipopolysaccharide-exposed rat lung pericytes. *J. Trauma* **62**, 89–93
40. Pace, E., Ferraro, M., Siena, L., Melis, M., Montalbano, A. M., Johnson, M., Bonsignore, M. R., Bonsignore, G., and Gjomarkaj, M. (2008) Cigarette smoke increases Toll-like receptor 4 and modifies lipopolysaccharide-mediated responses in airway epithelial cells. *Immunology* **124**, 401–411
41. Zoso, A., Sofoluwe, A., Bacchetta, M., and Chanson, M. (2019) Transcriptomic profile of cystic fibrosis airway epithelial cells undergoing repair. *Sci. Data* **6**, 240
42. Ikeda, K., Shaw-White, J. R., Wert, S. E., and Whitsett, J. A. (1996) Hepatocyte nuclear factor 3 activates transcription of thyroid transcription factor 1 in respiratory epithelial cells. *Mol. Cell Biol.* **16**, 3626–3636
43. Galambos, C., and deMello, D. E. (2007) Molecular mechanisms of pulmonary vascular development. *Pediatr. Dev. Pathol.* **10**, 1–17
44. De Val, S., and Black, B. L. (2009) Transcriptional control of endothelial cell development. *Dev. Cell* **16**, 180–195
45. Herriges, M., and Morrisey, E. E. (2014) Lung development: Orchestrating the generation and regeneration of a complex organ. *Development* **141**, 502–513
46. Sun, F., and Hu, K. (2015) Kruppel-like factor 4 inhibits the transforming growth factor-beta1-promoted epithelial-to-mesenchymal transition via downregulating plasminogen activator inhibitor-1 in lung epithelial cells. *Dis. Markers* **2015**, 473742
47. Gao, L., Qiu, H., Liu, J., Ma, Y., Feng, J., Qian, L., Zhang, J., Liu, Y., and Bian, T. (2017) KLF15 promotes the proliferation and metastasis of lung adenocarcinoma cells and has potential as a cancer prognostic marker. *Oncotarget* **8**, 109952–109961
48. Chen, Z., Zhang, Q., Wang, H., Li, W., Wang, F., Wan, C., Deng, S., Chen, H., Yin, Y., Li, X., Xie, Z., and Chen, S. (2017) Klf5 mediates odontoblastic differentiation through regulating dentin-specific extracellular matrix gene expression during mouse tooth development. *Sci. Rep.* **7**, 46746
49. Wang, P., Lu, Y. C., Li, Y. F., Wang, L., and Lee, S. C. (2018) Advanced glycation end products increase MDM2 expression via transcription factor KLF5. *J. Diabetes Res.* **2018**, 3274084
50. Matsumura, T., Suzuki, T., Aizawa, K., Munemasa, Y., Muto, S., Horikoshi, M., and Nagai, R. (2005) The deacetylase HDAC1 negatively regulates the cardiovascular transcription factor Kruppel-like factor 5 through direct interaction. *J. Biol. Chem.* **280**, 12123–12129
51. Wu, Q., Fu, C., Li, M., Li, J., Li, Z., Qi, L., Ci, X., Ma, G., Gao, A., Fu, X., A, J., An, N., Liu, M., Li, Y., King, J. L., *et al.* (2019) CINP is a novel cofactor of KLF5 required for its role in the promotion of cell proliferation, survival and tumor growth. *Int. J. Cancer* **144**, 582–594
52. Liu, X., Yin, S., Chen, Y., Wu, Y., Zheng, W., Dong, H., Bai, Y., Qin, Y., Li, J., Feng, S., and Zhao, P. (2018) LPSinduced proinflammatory cytokine expression in human airway epithelial cells and macrophages via NFkappaB, STAT3 or AP1 activation. *Mol. Med. Rep.* **17**, 5484–5491
53. Shu, S., Xu, Y., Xie, L., and Ouyang, Y. (2017) The role of C/EBPbeta phosphorylation in modulating membrane phospholipids repairing in LPS-induced human lung/bronchial epithelial cells. *Gene* **629**, 76–85
54. Hogmalm, A., Bry, M., and Bry, K. (2018) Pulmonary IL-1beta expression in early life causes permanent changes in lung structure and function in adulthood. *Am. J. Physiol. Lung Cell Mol. Physiol.* **314**, L936–L945
55. Yi, G., Liang, M., Li, M., Fang, X., Liu, J., Lai, Y., Chen, J., Yao, W., Feng, X., Hu, Lin, C., Zhou, X., and Liu, Z. (2018) A large lung gene expression study identifying IL1B as a novel player in airway inflammation in COPD airway epithelial cells. *Inflamm. Res.* **67**, 539–551
56. Sutterwala, F. S., Mijares, L. A., Li, L., Ogura, Y., Kazmierczak, B. I., and Flavell, R. A. (2007) Immune recognition of Pseudomonas aeruginosa mediated by the IPAF/NLRC4 inflammasome. *J. Exp. Med.* **204**, 3235–3245
57. Grandjean, T., Boucher, A., Thepaut, M., Monlezun, L., Guery, B., Faudry, E., Kipnis, E., and Dessein, R. (2017) The human NAIP-NLRC4-inflammasome senses the Pseudomonas aeruginosa T3SS inner-rod protein. *Int. Immunol.* **29**, 377–384
58. Storr, S. J., Safuan, S., Ahmad, N., El-Refaee, M., Jackson, A. M., and Martin, S. G. (2017) Macrophage-derived interleukin-1beta promotes human breast cancer cell migration and lymphatic adhesion *in vitro*. *Cancer Immunol. Immunother.* **66**, 1287–1294
59. Bell, S. M., Zhang, L., Xu, Y., Besnard, V., Wert, S. E., Shroyer, N., and Whitsett, J. A. (2013) Kruppel-like factor 5 controls villus formation and initiation of cytodifferentiation in the embryonic intestinal epithelium. *Dev. Biol.* **375**, 128–139
60. Schiller, K. R., Maniak, P. J., and O'Grady, S. M. (2010) Cystic fibrosis transmembrane conductance regulator is involved in airway epithelial wound repair. *Am. J. Physiol. Cell Physiol.* **299**, C912–C921

61. Okada, H., Yamada, M., Kamimoto, K., Kok, C. Y., Kaneko, K., Ema, M., Miyajima, A., and Itoh, T. (2018) The transcription factor Klf5 is essential for intrahepatic biliary epithelial tissue remodeling after cholestatic liver injury. *J. Biol. Chem.* **293**, 6214–6229
62. Chanchevalap, S., Nandan, M. O., McConnell, B. B., Charrier, L., Merlin, D., Katz, J. P., and Yang, V. W. (2006) Kruppel-like factor 5 is an important mediator for lipopolysaccharide-induced proinflammatory response in intestinal epithelial cells. *Nucleic Acids Res.* **34**, 1216–1223
63. Di Giammartino, D. C., Kloetgen, A., Polyzos, A., Liu, Y., Kim, D., Murphy, D., Abuhashem, A., Cavaliere, P., Aronson, B., Shah, V., Dephoure, N., Stadtfeld, M., Tsirigos, A., and Apostolou, E. (2019) KLF4 is involved in the organization and regulation of pluripotency-associated three-dimensional enhancer networks. *Nat. Cell Biol.* **21**, 1179–1190
64. Shen, B. Q., Finkbeiner, W. E., Wine, J. J., Mrsny, R. J., and Widdicombe, J. H. (1994) Calu-3: A human airway epithelial cell line that shows cAMP-dependent Cl- secretion. *Am. J. Physiol.* **266**, L493–L501
65. Cozens, A. L., Yezzi, M. J., Kunzelmann, K., Ohrui, T., Chin, L., Eng, K., Finkbeiner, W. E., Widdicombe, J. H., and Gruenert, D. C. (1994) CFTR expression and chloride secretion in polarized immortal human bronchial epithelial cells. *Am. J. Respir. Cell Mol. Biol.* **10**, 38–47
66. Fulcher, M. L., Gabriel, S., Burns, K. A., Yankaskas, J. R., and Randell, S. H. (2005) Well-differentiated human airway epithelial cell cultures. *Methods Mol. Med.* **107**, 183–206
67. Browne, J. A., Yang, R., Eggener, S. E., Leir, S. H., and Harris, A. (2016) HNF1 regulates critical processes in the human epididymis epithelium. *Mol. Cell Endocrinol.* **425**, 94–102
68. Dobin, A., Davis, C. A., Schlesinger, F., Drenkow, J., Zaleski, C., Jha, S., Batut, P., Chaisson, M., and Gingeras, T. R. (2013) Star: Ultrafast universal RNA-seq aligner. *Bioinformatics* **29**, 15–21
69. Liao, Y., Smyth, G. K., and Shi, W. (2014) featureCounts: an efficient general purpose program for assigning sequence reads to genomic features. *Bioinformatics* **30**, 923–930
70. Love, M. I., Huber, W., and Anders, S. (2014) Moderated estimation of fold change and dispersion for RNA-seq data with DESeq2. *Genome Biol.* **15**, 550
71. Raudvere, U., Kolberg, L., Kuzmin, I., Arak, T., Adler, P., Peterson, H., and Vilo, J. (2019) g:Profiler: a web server for functional enrichment analysis and conversions of gene lists (2019 update). *Nucleic Acids Res.* **47**, W191–W198
72. Carlson, M. (2019) *org.Hs.eg.db: Genome wide annotation for Human.* R package version 3.8.2, Bioconductor
73. Yang, Y., Goldstein, B. G., Chao, H. H., and Katz, J. P. (2005) KLF4 and KLF5 regulate proliferation, apoptosis and invasion in esophageal cancer cells. *Cancer Biol. Ther.* **4**, 1216–1221
74. Li, H., and Durbin, R. (2009) Fast and accurate short read alignment with Burrows-Wheeler transform. *Bioinformatics* **25**, 1754–1760
75. Zhang, Y., Liu, T., Meyer, C. A., Eeckhoute, J., Johnson, D. S., Bernstein, B. E., Nusbaum, C., Myers, R. M., Brown, M., Li, W., and Liu, X. S. (2008) Model-based analysis of ChIP-seq (MACS). *Genome Biol.* **9**, R137
76. Heinz, S., Benner, C., Spann, N., Bertolino, E., Lin, Y. C., Laslo, P., Cheng, J. X., Murre, C., Singh, H., and Glass, C. K. (2010) Simple combinations of lineage-determining transcription factors prime cis-regulatory elements required for macrophage and B cell identities. *Mol. Cell* **38**, 576–589
77. Quinlan, A. R., and Hall, I. M. (2010) BEDTools: A flexible suite of utilities for comparing genomic features. *Bioinformatics* **26**, 841–842
78. Yu, G., Wang, L. G., and He, Q. Y. (2015) ChIPseeker: An R/bioconductor package for ChIP peak annotation, comparison and visualization. *Bioinformatics* **31**, 2382–2383
79. Afgan, E., Baker, D., Batut, B., van den Beek, M., Bouvier, D., Cech, M., Chilton, J., Clements, D., Coraor, N., Gruning, B. A., Guerler, A., Hillman-Jackson, J., Hiltemann, S., Jalili, V., Rasche, H., *et al.* (2018) The galaxy platform for accessible, reproducible and collaborative biomedical analyses: 2018 update. *Nucleic Acids Res.* **46**, W537–W544
80. Diaferia, G. R., Balestrieri, C., Prosperini, E., Nicoli, P., Spaggiari, P., Zerbi, A., and Natoli, G. (2016) Dissection of transcriptional and cis-regulatory control of differentiation in human pancreatic cancer. *EMBO J.* **35**, 595–617
81. Leir, S. H., Holgate, S. T., and Lackie, P. M. (2003) Inflammatory cytokines can enhance CD44-mediated airway epithelial cell adhesion independently of CD44 expression. *Am. J. Physiol. Lung Cell Mol. Physiol.* **285**, L1305–L1311